BULLETIN OF THE POLISH ACADEMY OF SCIENCES
TECHNICAL SCIENCES, Vol. 70(5), 2022, Article number: e143108
DOI: 10.24425/bpasts.2022.143108

Specified weight cutting system for irregular solid material based on 3D scanning

Jiadong HE[1†], **Yafeng HUANG**[2†], **Xiao ZANG**[1], **and Yajun ZHANG**[1*]

[1] College of Mechanical and Electrical Engineering, Beijing University of Chemical Technology, Beijing, 100029, China
[2] Xi'an Modern Chemistry Research Institute, Xi'an, 710065, China

Abstract. A specified weight-cutting system for irregular solid materials such as rubber is important for industrial engineering. Currently, the workers' experience is used, which has low accuracy and efficiency. A specified weight cutting system for irregular solid material based on 3D scanning is proposed in this paper, which aims to overcome the inaccuracy and inefficiency of the manual cutting process. Firstly, the surface of the irregular solid material is scanned by a tracking 3D laser scanner, and a triangular mesh file is generated. Secondly, the defects of the 3D model are repaired by reverse engineering, and then the 3D model file of the irregular objects is generated. Finally, the cutting position of the specified weight solid material is calculated by the calculation algorithm in UG software. In short, this research creates a new method for processing data collected by the 3D scanner, by working jointly with multiple devices and software, facilitating the cutting of irregular solid materials with specified weights. Additionally, the system has the advantage of accuracy and efficiency over the experience of workers

Key words: specified weight; 3D scanning; reverse engineering; calculation algorithm.

1. INTRODUCTION

Solid materials cut with specified weight are needed before the production processes such as rubber mixing [1–3]. For regular solid materials such as cuboids and spheres, it can be calculated by the corresponding volume. However, the cutting position of irregular solid materials is difficult to obtain with a formula [4, 5]. Currently, the specified weight cutting of irregular solid materials is mainly based on a worker's experience, as shown in Fig. 1, which has low accuracy and efficiency. Hence, the manufacturing industry needs to develop a specified weight-cutting system for irregular solid materials.

Fig. 1. Specified weight cutting of irregular rubber realized by worker's experience

It is difficult to calculate the volume of irregular material with high efficiency [6]. The coordinate measuring machine [7] that appeared in the 1950s reconstructed the model through the reciprocating movement of a probe on the object surface; however, its acquisition speed is low and the device is expensive. Riccabona *et al.* [8] used ultrasound to scan irregular material and achieved acceptable 3D reconstruction results. However, a long scanning time resulted in insufficient efficiency. The 3D reconstruction based on computer vision deals mainly with the point cloud data of the object [9]. Dipanda *et al.* [10] used a single image for real-time dynamic measurement to reconstruct the 3D appearance of the object. This method had strict requirements for the relative position between the light source and the camera, and the height of the measured object was limited. Sun *et al.* [11] proposed a non-contact volume measurement method for irregular solid material based on 3D reconstruction technology. Although this method can reconstruct a 3D model more accurately and measure the volume of irregular solid materials, the equipment cost is high and there is no application in industry.

A 3D laser scanner can rebuild the 3D model of the measured object and various drawing data quickly. In recent years, 3D laser scanning has been applied in underwater manipulation [12], forensic engineering [13], and accurate measurement of earthwork [14]. It is only rebuilding the 3D model of the surface with a scan error and unnecessary points. There is no study focused on specified weight cutting of the irregular solid material.

Herein, a specified weight-cutting system for irregular solid materials based on 3D scanning is proposed in this paper. Firstly, the irregular solid material is scanned by a 3D scanner to obtain point cloud data. Secondly, a 3D model of the irregular

*e-mail: zhyj@mail.buct.edu.cn
† *Jiadong He and Yafeng Huang are co-first authors.*

Manuscript submitted 2022-07-20, revised 2022-08-28, initially accepted for publication 2022-09-19, published in October 2022.

solid material is reconstructed, and the model is repaired by reverse engineering. Finally, the cutting position of the specified weight of solid material is calculated by the algorithm proposed in Unigraphics NX(UG). The experimental object of this paper uses irregular rubber applied in the manufacture of tires. This paper innovatively develops a processing method for the data collected by the 3D scanner and uses multiple devices and software to operate jointly making the system achieve accurate and efficient cutting of irregular solid materials of specified weight.

2. 3D MODEL OF IRREGULAR SOLID MATERIAL

The irregular rubber was taken as an experimental subject for specified weight-cutting experiments. The 3D laser scanner consisting of a tracker and scanner, as shown in Fig. 2, which has completed the scanning path planning scans the irregular rubber. It is clamped by mechanical clamps and placed on the workbench yet does not include the bottom surface of the irregular rubber, and the scanned image contains a small part of the workbench. This system uses the FreeTrack optical dynamic tracking scanner as a 3D laser scanner, the scanning rate, scanning resolution, and measurement accuracy are 480,000 times/second, 0.05 mm, and 0.03 mm, respectively.

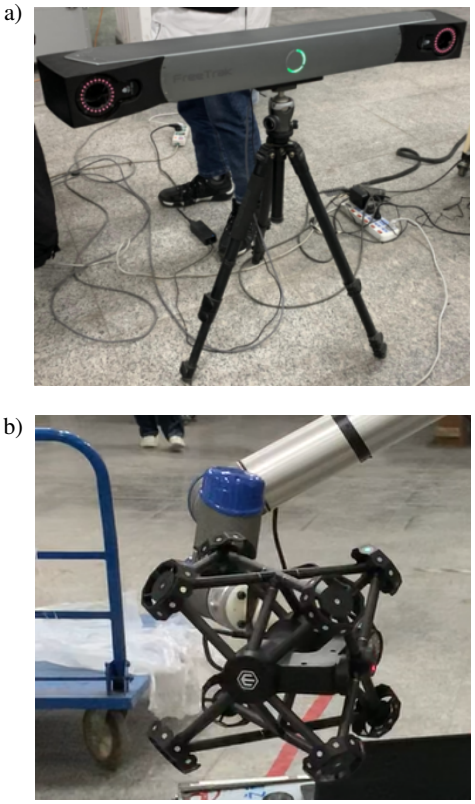

Fig. 2. a) Tracker and b) scanner of 3D laser scanner

In order to improve the automation of the system, a mechanical gripper is designed to clamp irregular rubber blocks. It is composed of vacuum suction cups, claws that prevent the falling of irregular rubber blocks, and a 3D vision camera for identifying and positioning irregular rubber blocks [15]. In the process of grasping and moving, the irregular rubber block is first sucked tightly by the vacuum suction cups. Then, the claws closed and wrapped the irregular rubber block, and the suction cups stop working. Finally, the mechanical gripper places the irregular rubber block on the workbench, as shown in Fig. 3. Finally, a 3D laser scanner is used to scan the surface of the irregular block, excluding the bottom surface in contact with the table, as shown in Fig. 4a.

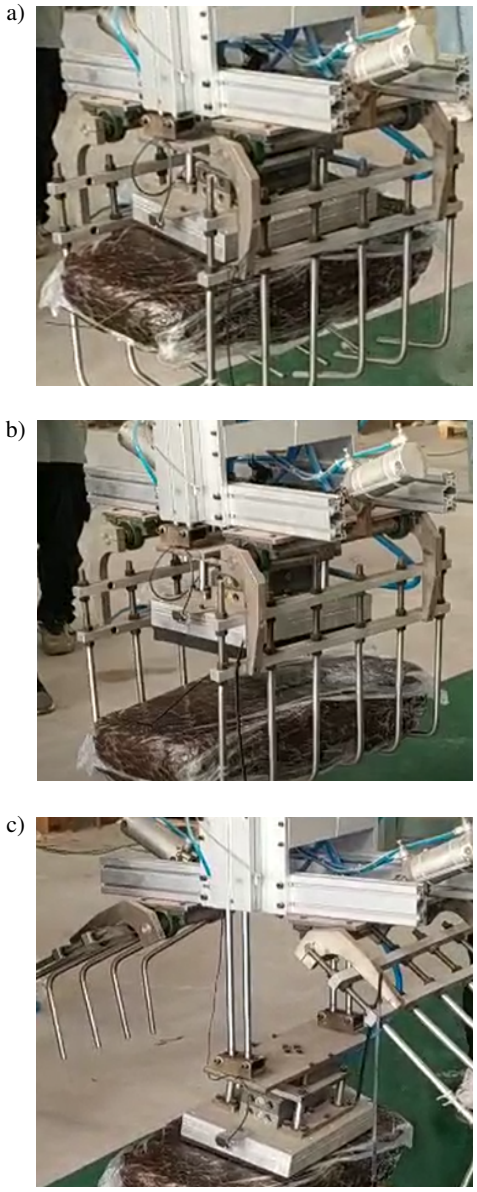

Fig. 3. The mechanical gripper clamps the irregular rubber block, a) vacuum adsorb clamps; b) prevent falling protector; c) placed on the workbench

The 3D laser scanner was scanning according to the planned path, and the scanning results include small sections of the workbench except the irregular rubber block model. The untreated point cloud result of the irregular rubber blocks achieved by the scanner is shown in Fig. 4b.

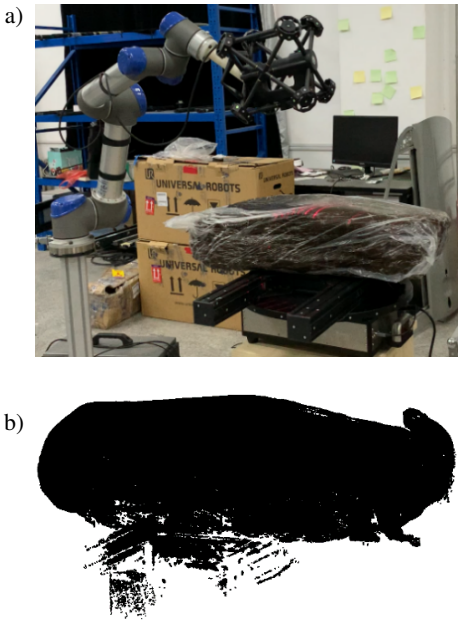

Fig. 4. The model of irregular rubber block scanned by the 3D laser scanner, a) placed on the workbench; b) untreated point cloud result

3. MODEL REPAIR BY REVERSE ENGINEERING

Reverse engineering is a product design technology reproduction process that carries out reverse analysis and research on a target product, so as to deduce and obtain the design elements such as the processing flow, organizational structure, functional characteristics and technical specifications of the product [16, 17]. This system uses Geomagic Wrap for scanning data processing, which can directly convert 3D scan data and imported files into 3D models for subsequent processing. The cutting process is visualized using UG, an interactive CAD/CAM (computer-aided design and computer-aided manufacturing) system from Siemens PLM Software, which facilitates the construction of complex solids and shapes.

In order to reconstruct a model of an irregular rubber block more accurately and generate the file that can be edited by UG, Geomagic Wrap is run to process the untreated point cloud result. Firstly, the untreated point cloud generated by the scanner is black. In order to observe the shape of the point cloud, it is necessary to color the point cloud, as shown in Fig. 5.

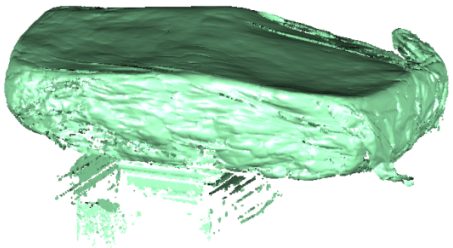

Fig. 5. The model of irregular rubber block scanned by the 3D laser scanner

Secondly, the redundant points are removed to obtain a simplified triangular mesh model of irregular rubber blocks, including external isolated points and unconnected point areas, as shown in Fig. 6, where external isolated points are the point with a large distance from the main point cloud in the model, its sensitive value is set at 85% and the unconnected point areas deviate from the area of the main point cloud more than 5%.

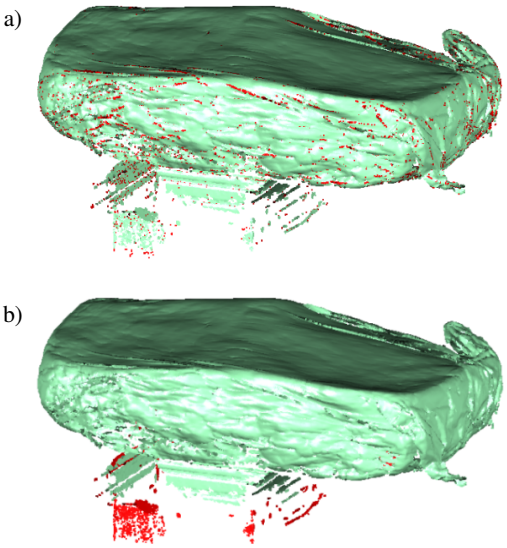

Fig. 6. Remove redundant points, a) remove external isolated points; b) remove unconnected point areas

Finally, the mesh is run doctor to repair model defects, including removing the workbench scanned by the scanner, simplifying the number of triangular meshes, filling all holes and the bottom surface of the irregular rubber block placed on the workbench, and supplementing accurate curves and surfaces, as shown in Fig. 7. Geomagic Wrap is a professional and powerful 3D scanning and analysis software and is widely used in architecture engineering, archaeology, industrial manufacturing, and other fields.

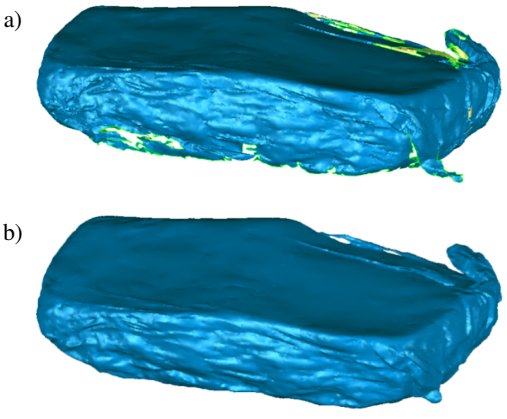

Fig. 7. Comparison before and after model repair. Irregular rubber block model: a) without filling and b) with filling

The .stl file is automatically transformed into the UG editable .stp file. Reverse engineering greatly improves the automation of the system. The model defects were repaired by reverse engineering as shown in Fig. 8.

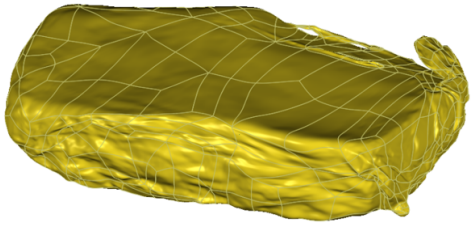

Fig. 8. The repaired model of the irregular rubber block

4. CUTTING POSITION OF THE SPECIFIED WEIGHT

The volume calculation of irregular rubber blocks is the key to specified weight cutting. As shown in Fig. 9a, calculus is used to calculate the volume of the irregular rubber block model in this system. The model of irregular rubber block is divided along the Y-axis, and the result is shown in Fig. 9b. Fitting the characteristic points of the two section curves is shown in Fig. 10.

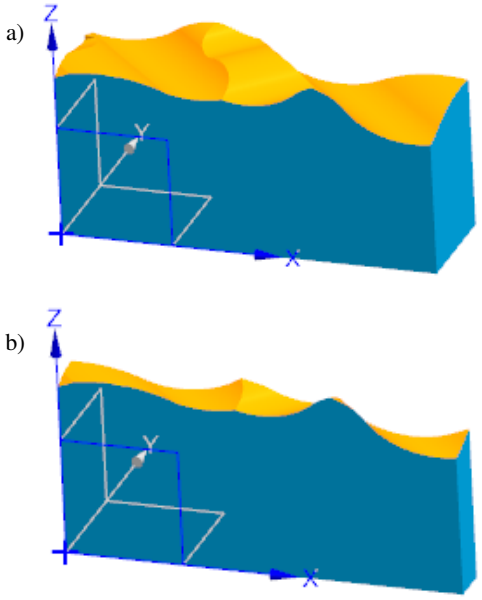

Fig. 9. Irregular rubber model segmented along Y-axis: a) before segmentation; b) after segmentation

The coordinate values of the feature points in Fig. 10 are $A_i(X_{ai}, Y_{ai}, Z_{ai})$, $B_i(X_{bi}, Y_{bi}, Z_{bi})$, $A_{i+1}(X_{ai+1}, Y_{ai+1}, Z_{ai+1})$. In addition, A_i', B_i', A_{i+1}' are the projection points of A_i, B_i and A_{i+1} on the $X0Y$ plane, respectively. The volume of the small trigonal prisms is expressed as:

$$\Delta V_i = \frac{(Z_{ai} + Z_{bi} + Z_{ai+1})}{3} \frac{(X'_{ai+1} - X'_{ai})(Y'_{bi} - Y'_{ai})}{2}, \quad (1)$$

where ΔV_i is the volume of the small trigonal prisms.

$$V_i = \sum_{i=1}^{n} \Delta V_i, \quad (2)$$

where V_i is the volume between two sections. The parameter n is the number of small trigonal prisms between two sections.

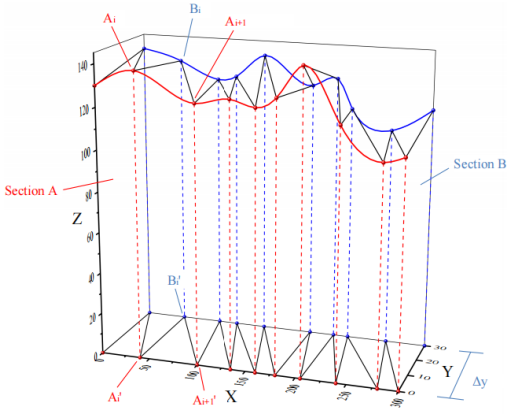

Fig. 10. Schematic drawing of a test piece and the location of wall thickness measurements

Therefore, the volume of the irregular rubber block is expressed as:

$$V = \sum_{i=1}^{j} V_i, \quad (3)$$

where V is the volume of the irregular rubber block. The parameter j is the number of volumes between sections segmented along the Y-axis.

Since the density of rubber blocks is known, hence, the volume of the irregular rubber block that required cutting was calculated by equation (4). To increase computational speed, the cut positions can be calculated quickly using a dichotomy based on the volume of the irregular rubber block. The position for specified weight cutting was calculated by the segmentation algorithm in the UG software, and the operation interface shown in Fig. 11. The "Trim body" and "Measure body" function commands of UG are run in Microsoft Visual Studio and the specified weight cutting program of an irregular block is written. The calculation process is shown in Fig. 12. Microsoft Visual Studio is a complete development toolset developed by Microsoft Corporation in the United States, which includes most of the tools needed throughout the software lifecycle, such as UML tools, code control tools, integrated development environment (IDE), etc. And the operating interface of this system is designed using Qt Designer, which is a tool for implementing the

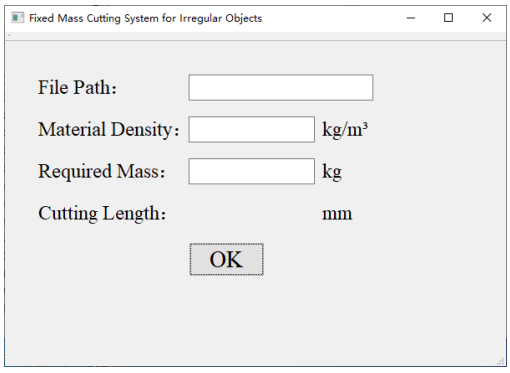

Fig. 11. The user interface of the specified weight cutting system for the irregular rubber block

UI interface of PyQt programs and is simple to operate, allowing complex interface designs to be completed by dragging and clicking.

$$V_{\text{need}} = \frac{M_{\text{need}}}{\rho}, \tag{4}$$

where V_{need} is the volume of an irregular rubber block that required cutting. The M_{need} is the weight needed to cut. And the ρ is the density of the rubber block.

In Fig. 12, $L_{\min}$ is the reference plane, usually taken as 0, $L_{\max}$ is the maximum length allowed to cut along the Y-axis, V_e is the allowable volume error, i is the cutting times, L is the final cutting position, μ is the density of the material, and M_r is the specified cutting quality, V_m is the measured volume, V_r is the required volume, N is the maximum number of cutting, and d is the length of the irregular rubber block along the Y-axis.

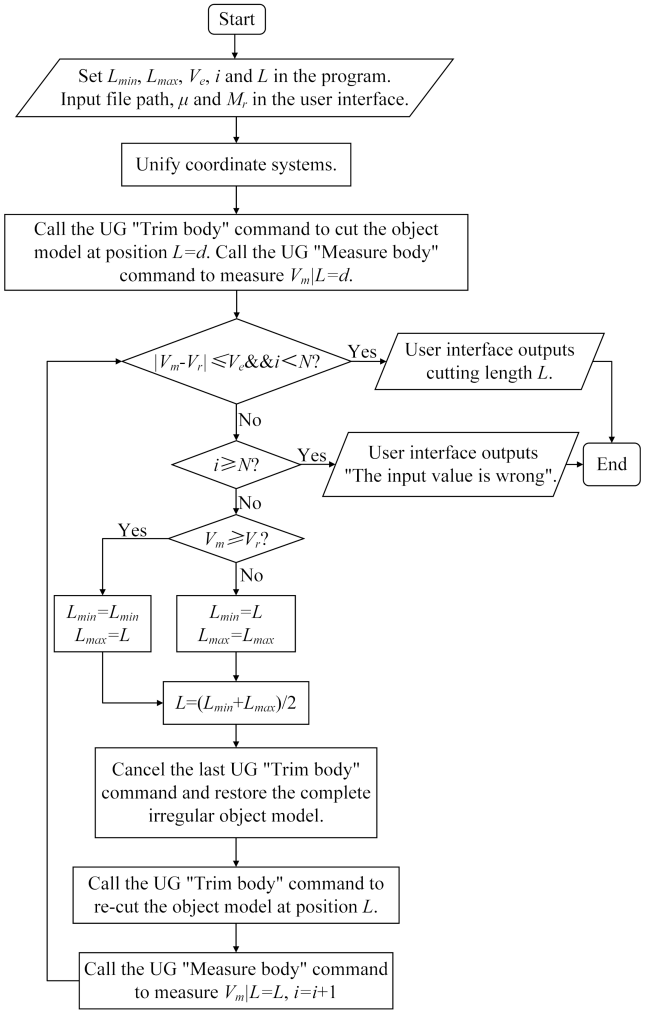

Fig. 12. Flow chart of cutting the specified weight

In order to verify the reliability of the cutting algorithm, specified weight-cutting simulation experiments were conducted 50 times, and the results are shown in Table 1. The error weights of 50 experiments are all between ±3.77 g, which proves that the cutting algorithm has good reliability.

Table 1
Results of repeated experiments

Number	M_r kg	M_r kg	M_e g	Number	M_r kg	M_r kg	M_e g
1	0.613	0.6121	–0.9	26	15.938	15.9363	–1.7
2	1.226	1.2262	0.2	27	16.551	16.5497	–1.3
3	1.839	1.838	–1	28	17.164	17.1622	–1.8
4	2.452	2.4541	2.1	29	17.777	17.7733	–3.7
5	3.065	3.0646	–0.4	30	18.39	18.3888	–1.2
6	3.678	3.6794	1.4	31	19.003	19.0006	–2.4
7	4.291	4.2877	–3.3	32	19.616	19.6153	–0.7
8	4.904	4.904	0	33	20.229	20.2258	–3.2
9	5.517	5.5151	–1.9	34	20.842	20.8399	–2.1
10	6.13	6.1314	1.4	35	21.455	21.4578	2.8
11	6.743	6.7397	–3.3	36	22.068	22.0709	2.9
12	7.356	7.3549	–1.1	37	22.681	22.6792	–1.8
13	7.969	7.9661	–2.9	38	23.294	23.2948	0.8
14	8.582	8.5821	0.1	39	23.907	23.9091	2.1
15	9.195	9.1953	0.3	40	24.52	24.5199	–0.1
16	9.808	9.807	–1	41	25.133	25.1296	–3.4
17	10.421	10.4191	–1.9	42	25.746	25.7451	–0.9
18	11.034	11.0351	1.1	43	26.359	26.3579	–1.1
19	11.647	11.6492	2.2	44	26.972	26.9690	–3
20	12.26	12.2598	–0.2	45	27.585	27.5825	–2.5
21	12.873	12.8727	–0.3	46	28.198	28.1995	1.5
22	13.486	13.4843	–1.7	47	28.811	28.8093	–1.7
23	14.099	14.0955	–3.5	48	29.424	29.4248	0.8
24	14.712	14.7094	–2.6	49	30.037	30.0358	–1.2
25	15.325	15.3233	–1.7	50	30.65	30.6497	–0.3

In Table 1, M_r and M_m are the required weight and the resulting weight after simulated cutting, respectively, and M_e is the error weight that is the D-value between M_r and M_m.

5. EXPERIMENT AND DISCUSSION

In calculating the cut position, a smooth plane was required as the reference plane, as shown in Fig. 13. Then, inputting the parameters on the user interface. For this experiment, the density of rubber is 950.3 kg/m^3 and the required weight is 18.6 kg as shown in Fig. 14. Finally, the calculated result is verified by UG, as shown in Fig. 15.

For the contingency of calculating the result, different weights of cutting and experimental results are shown in Fig. 16. The X-axis and Y-axis represent the desired weight M_{Required} and the cutting weight of the simulated experiment M_{Simulate}, respectively. The *ideal curves* represent cases that are always equal for M_{Required} and M_{Simulate}. During processing, the allowable error in weight is ±0.3 kg, which is Upper and Lower

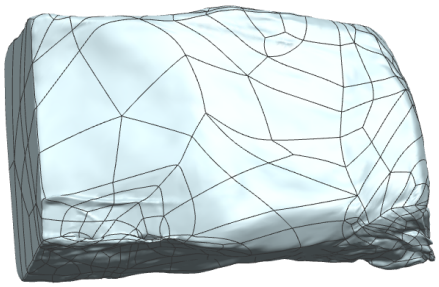

Fig. 13. Irregular rubber block model reference surface

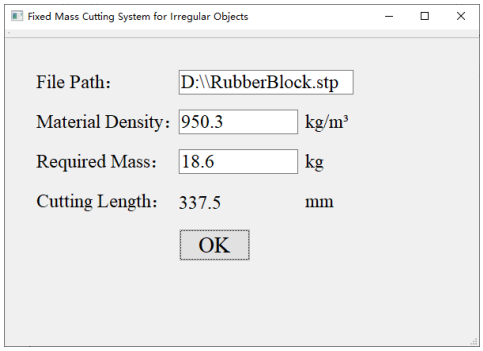

Fig. 14. The result of simulated specified weight cutting

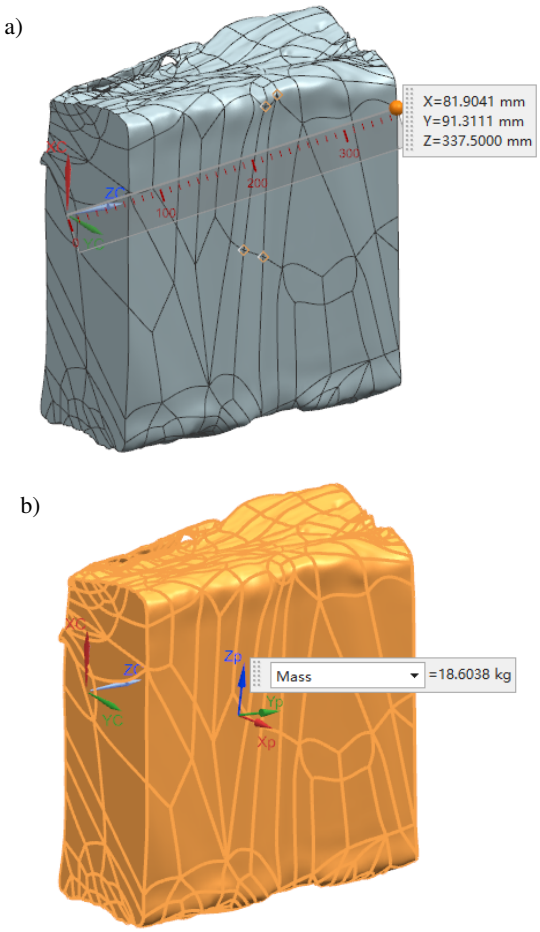

Fig. 15. Verification results of: a) cutting length and b) weight of specified weight cutting

limit of error margin. It can be seen in Fig. 16 that experimental curves are all distributed within the error range.

Significantly, reducing the number of triangular meshes and not scanning the bottom surface of irregular rubber blocks

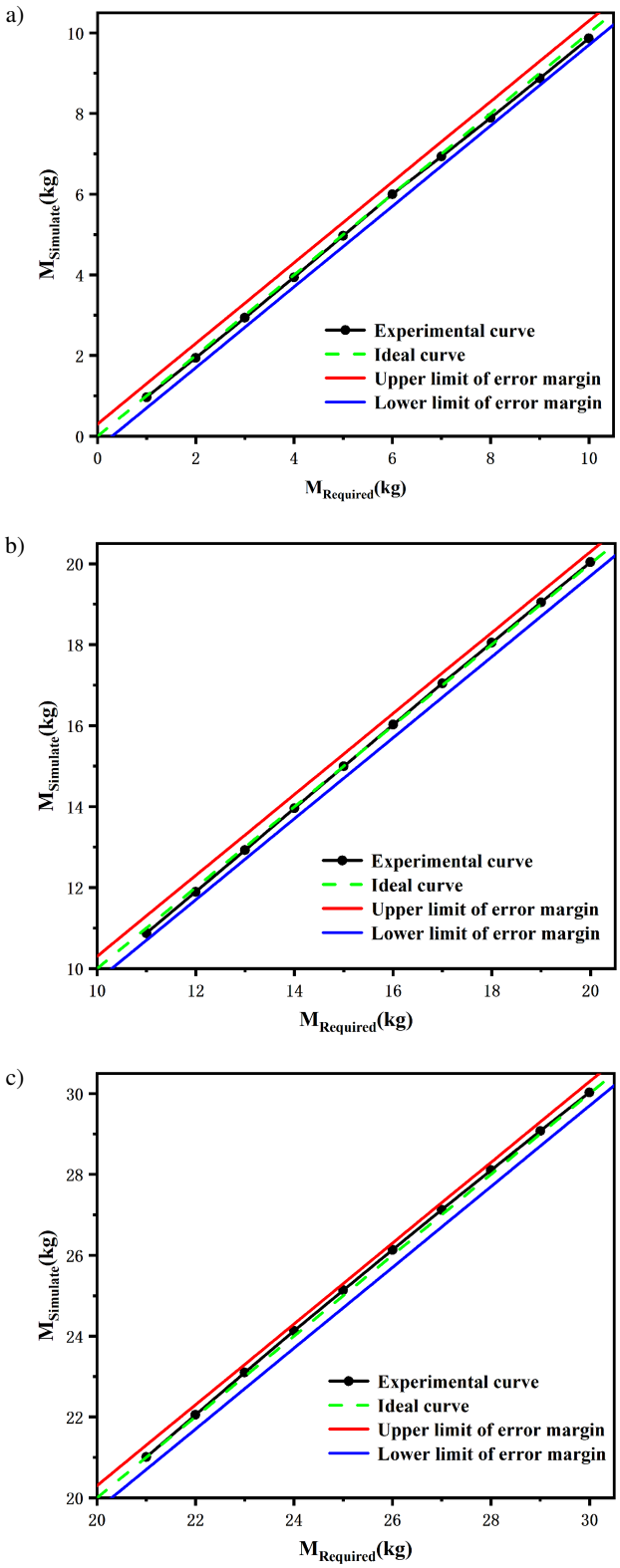

Fig. 16. The results of repeated experiments with the required masses of (a) 1–10 kg, (b) 11–20 kg and (c) 21–30 kg

Table 2
The error values caused by simplifying the mesh and filling the plane (mm^3)

Scanned area	Mesh processing	Volume	Volume error caused by simplifying the mesh	Volume error caused by filling the plane	Total volume error
All surfaces	No simplifying	37057			0
Except for the side	No simplifying	36764		–293	–293
Except for the bottom surface	No simplifying	35889		–1168	–1168
All surfaces	Simplifying	36984	–73		–73
Except for the side	Simplifying	37183	420	–293	127
Except for the bottom surface	Simplifying	36199	310	–1168	–858

Table 3
A comprehensive evaluation of scanning methods

Scanned area	Mesh processing	Complexity degree of progress	Consuming time of reverse engineering, s	Difficulty of fixture clamping
All surfaces	No simplifying	Complicated	563	Simple
Except for the side	No simplifying	Moderate	532	Difficult
Except for the bottom surface	No simplifying	Uncomplicated	924	Simple
All surfaces	Simplifying	Complicated	75	Simple
Except for the side	Simplifying	Moderate	67	Difficult
Except for the bottom surface	Simplifying	Uncomplicated	90	Simple

placed on the workbench can improve efficiency, but it will also lead to more errors. As shown in Table 2 where positive and negative values represent above and below standard volume values, respectively. To improve the calculation accuracy, the irregular rubber block was an error compensated in the calculation algorithm, and the compensated value was $-1.175 cm^3/mm$.

The scanning efficiency of this system is also an important factor affecting industrial applications. Therefore, the comprehensive comparison is made from process complexity, time of reverse engineering and clamping difficulty, as shown in Table 3. The results demonstrated that it was the best scheme for industrial applications by reducing the number of triangular meshes and not scanning the bottom surface of the irregular rubber block placed on the workbench.

6. CONCLUSIONS

A specified weight-cutting system for irregular solid material based on 3D scanning is presented in this paper. And the irregular rubber block is used as an experimental subject. The results show that the system satisfies the rigorous requirements of ± 300 g. It overcomes the disadvantages of the worker's experience and improves the accuracy and efficiency of cutting.

At present, this system is used in the rubber processing industry. We will continue to optimize the algorithm to improve the calculation efficiency and accuracy of the system and expand the application scope of this system in other industries with similar needs.

REFERENCES

[1] A. Hasan, Rochmadi, H. Sulistyo, and S. Honggokusumo, "Rubber mixing process and its relationship with bound rubber and crosslink density," in *IOP Conf. Ser.: Mater. Sci. Eng. Global Conference on Polymer and Composite Materials (PCM)*, 2017, vol. 213, p. 012048, doi: 10.1088/1757-899x/213/1/012048.

[2] K.G. Alahapperuma, "Optimize technical properties with master batch blends in RSS/Scrap rubber tire retread compounds," in *Moratuwa Engineering Research Conference (MERCon)/7th International Multidisciplinary Engineering Research Conference*, 2021, pp. 549–554, doi: 10.1109/mercon52712.2021.9525745.

[3] Y. Nakanishi, K. Mita, K. Yamamoto, K. Ichino, and M. Takenaka, "Effects of mixing process on spatial distribution and coexistence of sulfur and zinc in vulcanized EPDM rubber," *Polymer*, vol. 218, p. 7, Mar 2021, doi: 10.1016/j.polymer.2021.123486.

[4] S.R. Silva, M. Almeida, I. Condotta, A. Arantes, C. Guedes, and V. Santos, "Assessing the feasibility of using kinect 3D images to predict light lamb carcasses composition from leg volume," *Animals*, vol. 11, no. 12, p. 3595, Dec 2021, doi: 10.3390/ani11123595.

[5] Y.H. Fan, Y.S. Xu, Z.P. Hao, and J.Q. Lin, "Dynamic behavior description and three-dimensional cutting simulation of SiCp/Al composites with high volume fraction," *J. Manuf. Process.*, vol. 77, pp. 174–189, May 2022, doi: 10.1016/j.jmapro.2022.03.015.

[6] T.T.M. Huynh, L. TonThat, and S.V.T. Dao, "A vision-based method to estimate volume and mass of fruit/vegetable: Case study of sweet potato," *Int. J. Food Prop.*, vol. 25, no. 1, pp. 717–732, Dec 2022, doi: 10.1080/10942912.2022.2057528.

[7] J. Bryan and D. Carter, "Design of a new error-corrected co-ordinate measuring machine," *Precis. Eng.*, vol. 1, no. 3, pp. 125–128, 1979, doi: 10.1016/0141-6359(79)90036-9.

[8] M. Riccabona, T.R. Nelson, D.H. Pretorius, and T.E. Davidson, "Distance and volume measurement using 3-dimensional ultrasonography," *J. Ultrasound Med.*, vol. 14, no. 12, pp. 881–886, Dec 1995, doi: 10.7863/jum.1995.14.12.881.

[9] W. Blaszczak-Bak, Z. Koppanyi, and C. Toth, "Reduction Method for Mobile Laser Scanning Data," *ISPRS Int. J. Geo-Inf.*, vol. 7, no. 7, p. 285, Jul 2018, doi: 10.3390/ijgi7070285.

[10] A. Dipanda and S. Woo, "Towards a real-time 3D shape reconstruction using a structured light system," *Pattern Recognit.*, vol. 38, no. 10, pp. 1632–1650, Oct 2005, doi: 10.1016/j.patcog.2005.01.006.

[11] Y.T. Sun, T.W. Yang, X.Q. Cheng, and Y. Qin, "Volume measurement of moving irregular objects using linear laser and camera," in *8th IEEE Annual International Conference on Cyber Technology in Automation, Control, and Intelligent Systems (IEEE-CYBER)*, 2018, pp. 1288–1293, doi: 10.1109/CYBER.2018.8688302.

[12] A. Palomer, P. Rada, D. Youakim, D. Ribas, J. Forest, and Y. Petillot, "3D laser scanner for underwater manipulation," *Sensors*, vol. 18, no. 4, p. 1086, Apr 2018, doi: 10.3390/s18041086.

[13] C.S. Park, H.P. Jeon, K.S. Choi, J.P. Kim, and N.K. Park, "Application of 3D laser scanner to forensic engineering," *J. Forensic Sci.*, vol. 63, no. 3, pp. 930–934, May 2018, doi: 10.1111/1556-4029.13632.

[14] X.G. Feng, M. Li, and J.X. Liu, "Study on application of terrestrial 3D laser scanning technology in the calculation of the fine earthwork," in *Applied Mechanics and Materials: Advances in Civil and Industrial Engineering IV*, vol. 580, pp. 2833–2837, 2014, , doi: 10.4028/www.scientific.net/amm.580-583.2833.

[15] D. Xiao, M.M. Song, B.K. Ghosh, N. Xi, T.J. Tarn, and Z.Y. Yu, "Real-time integration of sensing, planning and control in robotic work-cells," *Control Eng. Pract.*, vol. 12, no. 6, pp. 653–663, Jun 2004, doi: 10.1016/s0967-0661(03)00146-1.

[16] U.J. Botero *et al.*, "Hardware trust and assurance through reverse engineering: A tutorial and outlook from image analysis and machine learning perspectives," *ACM J. Emerg. Technol. Comput. Syst.*, vol. 17, no. 4, p. 62, Oct. 2021, doi: 10.1145/3464959.

[17] I. Rojek, D. Mikolajewski, J. Nowak, Z. Szczepanski, and M. Macko, "Computational intelligence in the development of 3D printing and reverse engineering," *Bull. Pol. Acad. Sci. Tech. Sci.*, vol. 70, no. 1, p. e140016, Feb. 2022, doi: 10.24425/bpasts.2021.140016.